

See discussions, stats, and author profiles for this publication at: <https://www.researchgate.net/publication/227695567>

# Proton transfer dynamics and N–H bond lengthening in N–H···N model systems: A solid-state NMR study

ARTICLE *in* MAGNETIC RESONANCE IN CHEMISTRY · DECEMBER 2001

Impact Factor: 1.18 · DOI: 10.1002/mrc.957

---

CITATIONS

21

---

READS

34

2 AUTHORS, INCLUDING:



[Ann Mcdermott](#)

Columbia University

100 PUBLICATIONS 4,012 CITATIONS

SEE PROFILE

# Proton transfer dynamics and N—H bond lengthening in N—H···N model systems: a solid-state NMR study

Xiang-jin Song,<sup>†</sup> and Ann E. McDermott\*

Department of Chemistry, Columbia University, New York, New York 10027, USA

Received 12 June 2001; Accepted 20 August 2001

Hydrogen-bonded pairs of the 2-methylimidazolium cation and 2-methylimidazole are expected to have matched  $pK_a$  values, owing to chemical symmetry. These structures serve as models for enzyme active sites. Several crystalline salts of this system were prepared and characterized by crystallography and solid-state NMR. Short N···N distances are observed ( $\sim 2.65$  Å), and fast ( $>10^5$  s<sup>-1</sup>) proton transfer through the N—H···N bridge was suggested by NMR lineshape measurements at temperatures from 200 to 320 K. The equilibrium constants for these transfer processes were found to differ from unity, and to be strongly temperature and counter-ion dependent. For the perchlorate salt, the proton is observed to be mainly attached to one of the bridge nitrogens across this temperature range, for the iodide salt, the proton is substantially delocalized on to both bridging nitrogens across the temperature range. Interestingly, for the chloride and bromide salts, a temperature-dependent equilibrium constant is observed, with equal populations of the two isomers in rapid exchange at room temperature and an effectively trapped proton (or very strong population of one isomer) at 200 K. This temperature-dependent equilibrium constant indicates that the proton transfer is associated with an enthalpy of the order the 20 kJ mol<sup>-1</sup>. This study underscores the power of NMR spectroscopy to account for protons, and the important influence of remote ionic interactions on proton transfer coordinates. Copyright © 2001 John Wiley & Sons, Ltd.

**KEYWORDS:** NMR; solid-state NMR; <sup>15</sup>N NMR; x-ray crystal structure; dipolar chemical shift spectroscopy; N—H···N hydrogen bonding systems; imidazole; counterion effects; low barrier hydrogen bonds; symmetric hydrogen bonds

## INTRODUCTION

N—H···N hydrogen bonds appear in many important biological systems. For example, the His-12–His-119 pair in ribonuclease has been hypothesized to form a short, strong hydrogen bond to facilitate the free movement of protons at the active site.<sup>1</sup> In human cyto-megaloviral (hCMV) protease, His-157, which replaces Asp in other serine proteases, functions as a member of a so-called 'catalytic triad' with His-63 and Ser-132.<sup>2</sup> We are interested in the proton position, dynamics and potential surface for N—H···N systems.

Although N—H···N systems are not as well characterized as O—H···O systems; important studies of 'proton sponges',<sup>3–7</sup> linear NHN bridge compounds<sup>8,9</sup> and other interesting compounds<sup>10–15</sup> have been reported. The better studied O—H···O systems provide us with hypotheses about hydrogen bonding. For example, the O—H covalent bond length varies by as much as 0.3 Å as a function of

the hydrogen bond<sup>16</sup> particularly for very short hydrogen bonds, in which donors and acceptors are  $pK_a$  matched.<sup>17</sup> Perturbation of N—H bond lengths in hydrogen bonds is also known, but is much smaller ( $<0.05$  Å).<sup>17–19</sup> An unusually long N—H bond (1.17 Å) and a short NHN hydrogen bond (N···N 2.56 Å) has been shown for one metal-containing case, possibly implying a single well potential for the proton.<sup>8</sup> The effect of the environment and counterion in controlling the details of the hydrogen bond has also been explored. Proton transfer rates through the NHN bridge and the symmetry of the potential wells can be altered by substitutions or counter ions, as has been indicated experimentally<sup>7–9,20,21</sup> and through computational studies.<sup>8,9,22–24</sup>

To investigate these points in more detail, and to study a case closely mimicking protein active sites, a series of model compounds involving coupled bis-imidazole hemi-cations, with a variety of counter anions, were designed, synthesized and characterized. Two identical aromatic rings provide the possibility of matched proton affinities in the bridge. Since the samples differ only in their counter anions, the comparison of their dynamic and structural properties, based on solid-state NMR measurements, may help us understand more about the role of counterions in N—H···N hydrogen bonds.

\*Correspondence to: A. E. McDermott, Department of Chemistry, Columbia University, New York, New York 10027, USA.  
E-mail: aem5@columbia.edu

<sup>†</sup>Present address: Department of Biochemistry and Biophysics, University of Pennsylvania, Philadelphia, Pennsylvania 19104, USA.

Contract/grant sponsor: National Institutes of Health;  
Contract/grant number: GM49964.

## EXPERIMENTAL

Compounds involving an imidazole imidazolium complex were synthesized and their structures were determined in previous work by Quick and Williams<sup>11</sup> and Therrien and Beauchamp.<sup>25</sup> In this work, 10%  $^{15}\text{N}$ -labeled 2-methylimidazole and 90% natural abundance material was used as a mixture.

The 2-methylimidazole 2-methylimidazolium perchlorate  $[\text{2-Me-Im.H.2-Me-Im}]^+\text{ClO}_4^-$ , crystal was obtained by dissolving the 2-methylimidazole powder (10%  $^{15}\text{N}$  enriched) in  $\text{HClO}_4$  (70 wt% in water, Aldrich) with a mole ratio of 2:1, followed by slow evaporation in a bottle with  $\text{P}_2\text{O}_5$  powder at  $4^\circ\text{C}$  for 1–2 days. The crystal was then lyophilized overnight and stored in a dry atmosphere. The chloride crystal  $[\text{2-MeIm}_2\text{H}]^+\text{Cl}^-$  was obtained by dissolving the 2-methylimidazole powder (10%  $^{15}\text{N}$  enriched) in  $\text{HCl}$  (37.5 wt% in water, Aldrich) with a mole ratio of 2:1, followed by slow evaporation in a bottle with  $\text{P}_2\text{O}_5$  powder for 1–2 days. The crystal was then lyophilized overnight and stored in a dry atmosphere. The bromide crystal  $[\text{2-MeIm}_2\text{H}]^+\text{Br}^-$  was obtained by dissolving the 2-methylimidazole powder (10%  $^{15}\text{N}$  enriched) in  $\text{HBr}$  (48 wt% in water, Aldrich) with a mole ratio of 2:1, followed by slow evaporation in a bottle with  $\text{P}_2\text{O}_5$  powder for 1–2 days. The crystal was then lyophilized overnight and stored in a dry atmosphere. The iodide crystal  $[\text{2-MeIm}_2\text{H}]^+\text{I}^-$  was obtained by dissolving the 2-methylimidazole powder (10%  $^{15}\text{N}$  enriched) in  $\text{HI}$  (55 wt%, in water, Aldrich) with a mole ratio of 2:1, followed by slow evaporation in a bottle with  $\text{P}_2\text{O}_5$  powder at  $4^\circ\text{C}$  for 1–2 days. The crystal was then lyophilized overnight and stored in a dry atmosphere. All the samples were strongly water sensitive, and were handled in a glove-box. Magic angle spinning (MAS) NMR rotors were sealed. The iodide sample was stored dark conditions.  $(2\text{MI})_2\text{HClO}_4$ ,  $(2\text{MI})_2\text{HCl}$ ,  $(2\text{MI})_2\text{HBr}$ ,  $(2\text{MI})_2\text{HI}$  will be used to refer to these samples in the following discussion and figures.

X-ray diffraction confirmed the presence of intermolecular  $\text{N}-\text{H}\cdots\text{N}$  hydrogen bonds in these samples. All the measurements were conducted on a Bruker P4 x-ray diffractometer, equipped with a SMART CCD detector. The  $\text{N}\cdots\text{N}$  distances determined in the four compounds are shown in Table 1.

All solid-state NMR measurements were performed on a Bruker DRX300wb spectrometer, with a Bruker wide board 89 mm double resonance probe, operating at 30.41 MHz for  $^{15}\text{N}$ . The  $^{15}\text{N}$  chemical shift values were relative to liquid ammonia at  $-50^\circ\text{C}$ . 1D VT  $^{15}\text{N}$  cross-polarization (CP)/MAS NMR spectra were measured with a sample spinning speed

of 4500 Hz. The repetition delay was 20 s, owing to the long  $T_1$  of these compounds ( $>7$  s). The  $^1\text{H}$   $90^\circ$  proton pulse length was  $2.8\ \mu\text{s}$ . Cross-polarization was performed with a contact time of 5.0 ms. The temperature range was 190–350 K (as indicated). A two-pulse phase modulation (TPPM) pulse sequence 26 was used for decoupling. 2D  $^{15}\text{N}$  exchange experiments were performed with a pulse sequence analogous to that used for NOESY spectroscopy in solution NMR.<sup>27,28</sup> The only significant modification was the use of cross-polarization for signal enhancement (as described above).<sup>29–33</sup> The 2D  $2\phi$ -DipShift experiment was used to resolve dipolar coupling and chemical shift interactions into two different dimensions<sup>34–38</sup> with a spinning speed of 2688 Hz. Data fitting was performed as described elsewhere.<sup>33</sup>

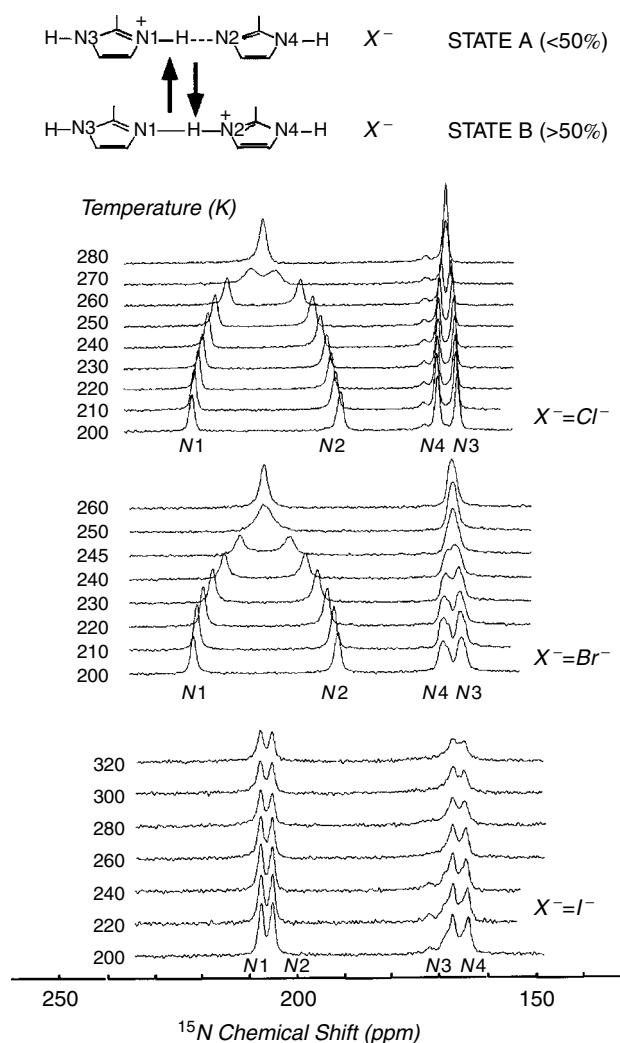


**Figure 1.** VT CP/MAS  $^{15}\text{N}$  NMR spectra for  $(2\text{MI})_2\text{HCl}$ ,  $(2\text{MI})_2\text{HBr}$  and  $(2\text{MI})_2\text{HI}$ . Chemical shifts are relative to liquid ammonia ( $-50^\circ\text{C}$ ). The nitrogens in the  $\text{NHN}$  bridges give rise to the peaks centered at 190–225 ppm. Of these two peaks, the downfield peak is the fast-limit averaged signal of the nitrogen (N-1) and the high-field peak is the fast-limit averaged signal of the nitrogen (N-2). The two peaks centered around 161–167 ppm were from the other two outer, non-bridging nitrogen sites. Chemical shifts are listed in Table 2.

**Table 1.**  $\text{N}\cdots\text{N}$  distances in 2-methylimidazole cations

Cation	$\text{N}\cdots\text{N}$ ( $\text{\AA}$ )
$(2\text{MI})_2\text{HClO}_4$	2.683
$(2\text{MI})_2\text{HCl}$	2.654
$(2\text{MI})_2\text{HBr}$	2.665
$(2\text{MI})_2\text{HI}$	2.666

## RESULTS AND DISCUSSION

The compounds under investigation exhibit N...N distances of 2.65–2.68 Å, which is short in comparison with other N...N distances (Table 1). This result is consistent with the notion that systems with matched proton affinities often exhibit short hydrogen bonds. A 'critical bond length'<sup>5</sup> has been defined for hydrogen-bonded systems, above which the proton is trapped and the potential function is asymmetric, and below which a single well is expected and a 'continuum' is observed in the IR spectrum (from 3000 to below 200 cm<sup>-1</sup>). For N—H...N systems this critical length is expected to be 2.65 Å; our compounds are therefore near the lengths where single well behaviour might be expected.<sup>33</sup> The compounds exhibit hydrogen bonds that are 'in-line' or linear, and are not bifurcated. In establishing the position and the dynamic characteristics of the proton, we used solid-state NMR measurements. In contrast with x-ray diffraction, the NMR spectra can be revealing in terms of the proton position, as described below.

Figure 1 and Table 2 summarize the <sup>15</sup>N CP variable-temperature spectra of the imidazole hemi-acids of bromide, iodide and chloride and perchlorate salt.<sup>33</sup> <sup>15</sup>N isotropic shifts can be used to deduce the proton positions. Non-protonated nitrogens in imidazole groups are usually associated with <sup>15</sup>N isotropic shifts of ~245 ppm, but when short hydrogen bonding is involved the shift can be as low as 225 ppm. Protonated nitrogens in imidazole groups are usually associated with <sup>15</sup>N isotropic shifts of ~165 ppm, but when short hydrogen bonding is involved the shift can be as high as 185 ppm.<sup>39–41</sup> For all compounds, the NMR spectra confirm the assumption that a single equivalent of HX is present for two equivalents of Im. Two lines are consistently seen in the range 155–170 ppm for each compound at low temperatures.

These are assumed to be associated with the outer N—H positions. Some of these lines are further broadened or split, possibly owing to low site symmetry or isotope effects. Two lines associated with the bridging position are also seen at low temperature in each case. For some of the spectra taken at warmer temperatures the bridge lines and the outer lines have merged to form a single line of higher intensity. The nitrogen lines associated with the bridge positions can be analyzed to determine the ionization state of the dimer and are consistent with a diimidazole monocation in every case, as expected.

For the perchlorate salt, the <sup>15</sup>N NMR spectra clearly suggest that one ring is cationic and the second neutral: the observation of one nitrogen line at 217 ppm and the other at 197 ppm suggest that the proton is associated with one ring specifically. The short N...N hydrogen bond between the two rings has apparently perturbed the shifts somewhat. For the iodide salt, the spectra suggest that each ring is associated with a half occupancy of the proton. The observation of two shifts in the range 206–210 ppm can be best explained by an averaged environment: rapid proton transfer in the N—H...N bridge results in two hemi-protonated nitrogens. In both cases there is no evidence for temperature dependence of the equilibrium constant for the proton.

For the chloride and bromide salts, the line positions are strongly dependent upon temperature for the bridging nitrogens. At high temperatures the bridging nitrogens appear at averaged chemical shifts (208–210 ppm), suggestive of facile proton transfer in the bridge with equal populations, whereas at low temperatures two peaks are seen at ~223 and ~191 ppm, suggestive of a largely 'trapped' proton, or a fast-limit process with a very strong preferences for

**Table 2.** Temperature-dependent <sup>15</sup>N chemical shifts for the bridging nitrogens (ppm, relative to liquid ammonia at -50 °C)

T (K)	(2MI) <sub>2</sub> HCl <sup>a</sup>		(2MI) <sub>2</sub> HBr <sup>a</sup>		(2MI) <sub>2</sub> HI <sup>a</sup>		T (K)	(2MI) <sub>2</sub> HClO <sub>4</sub> <sup>a</sup>	
280	<b>208.14</b> (59.7)		—		<b>209.30</b> (51.5)	<b>206.71</b> (54.3)	335	No signal	
270	<b>210.72</b> (135)	<b>205.19</b> (127)	—		—		315	<b>214.63</b> (51.5)	<b>200.89</b> (56.9)
260	<b>215.81</b> (51.5)	<b>199.84</b> (57.0)	<b>207.49</b> (65.1)		<b>209.30</b> (48.8)	<b>206.62</b> (48.8)	295	<b>215.88</b> (43.4)	<b>199.55</b> (43.4)
250	<b>218.48</b> (46.1)	<b>197.17</b> (51.5)	<b>207.85</b> (127.5)		—		275	<b>216.59</b> (38.0)	<b>198.75</b> (38.0)
(245)	—		<b>212.93</b> (78.7)	<b>201.78</b> (92.2)	—		255	<b>217.12</b> (38.0)	<b>198.22</b> (40.7)
240	<b>220.09</b> (46.0)	<b>195.56</b> (46.0)	<b>216.32</b> (59.7)	<b>198.48</b> (62.4)	<b>209.30</b> (46.1)	<b>206.62</b> (48.8)	235	<b>217.13</b> (38.0)	<b>197.57</b> (40.7)
230	<b>221.31</b> (43.4)	<b>194.13</b> (48.8)	<b>218.82</b> (48.8)	<b>195.81</b> (57.0)	—				
220	<b>222.23</b> (43.4)	<b>193.15</b> (48.8)	<b>220.96</b> (43.4)	<b>193.58</b> (48.8)	<b>209.21</b> (48.8)	<b>206.62</b> (46.1)			
210	<b>223.03</b> (40.1)	<b>192.08</b> (46.1)	<b>222.3</b> (43.4)	<b>192.06</b> (48.8)	—				
200	<b>223.75</b> (40.7)	<b>191.28</b> (46.1)	<b>223.11</b> (43.4)	<b>191.26</b> (48.8)	<b>209.12</b> (48.8)	<b>206.62</b> (46.1)			

<sup>a</sup> Peak chemical shifts are given in bold with FWHM linewidths in parentheses.

one of the two ionization states. The dramatic temperature-dependence of the spectrum is suggestive of temperature dependent proton transfer in the  $N-H \cdots N$  bridges. The temperature dependence of the spectra for the chloride and bromide salts appears to achieve coalescence at first glance, but do not fit to a classical intermediate lineshape expression, in particular since no line broadening is observed. The experimental lineshapes cannot be simulated using simple two-site exchange with equally populated sites. An illustration of a 'classic' intermediate exchange is shown in Fig. 2(a). Near the coalescence temperature, dramatic broadening is seen for the simulation, but this was not observed experimentally for any of the four compounds.

The most likely explanation for the bromide and chloride spectra is that the proton motion is in the fast limit at all temperatures and that the split peak results from differences in population of the two ionization configurations, rather than from a slow proton transfer rate.<sup>33</sup> If the transfer rate is in the fast limit, then both peak shifts are expected to reflect population weighted

averages of the shifts for protonated and deprotonated nitrogens, and spectra such as ours can be explained [Fig. 2(b)]. If the rates are apparently fast on the NMR time-scale at all temperatures, the estimated barrier heights of the proton transfer for our  $N-H \cdots N$  systems would be approximately  $\leq 8 \text{ kcal mol}^{-1}$  ( $1 \text{ kcal} = 4.184 \text{ kJ}$ ). This is unsurprising, particularly for a short and largely in-line hydrogen bond (angles vary from  $140$  to  $170^\circ$ ). Fast proton transfer for these compounds is expected based on many previous calculations.<sup>42–44</sup> An analysis of proton sponge as polystyrene or phthalocyanine compounds based upon an analogous fast-limit model was reported previously.<sup>45–47</sup> This phenomenon was described<sup>46</sup> as 'two-state exchange in the presence of molecular symmetry,' referring to the fact that the exchange equilibrium is disturbed from unity by the intermolecular interactions in solid-state samples. Indeed, in the solid state, the rigid structure imposes an important perturbation and the hydrogen bonding symmetry is typically lowered by crystal packing forces. Alternatively these spectra could be designated by 'rapid

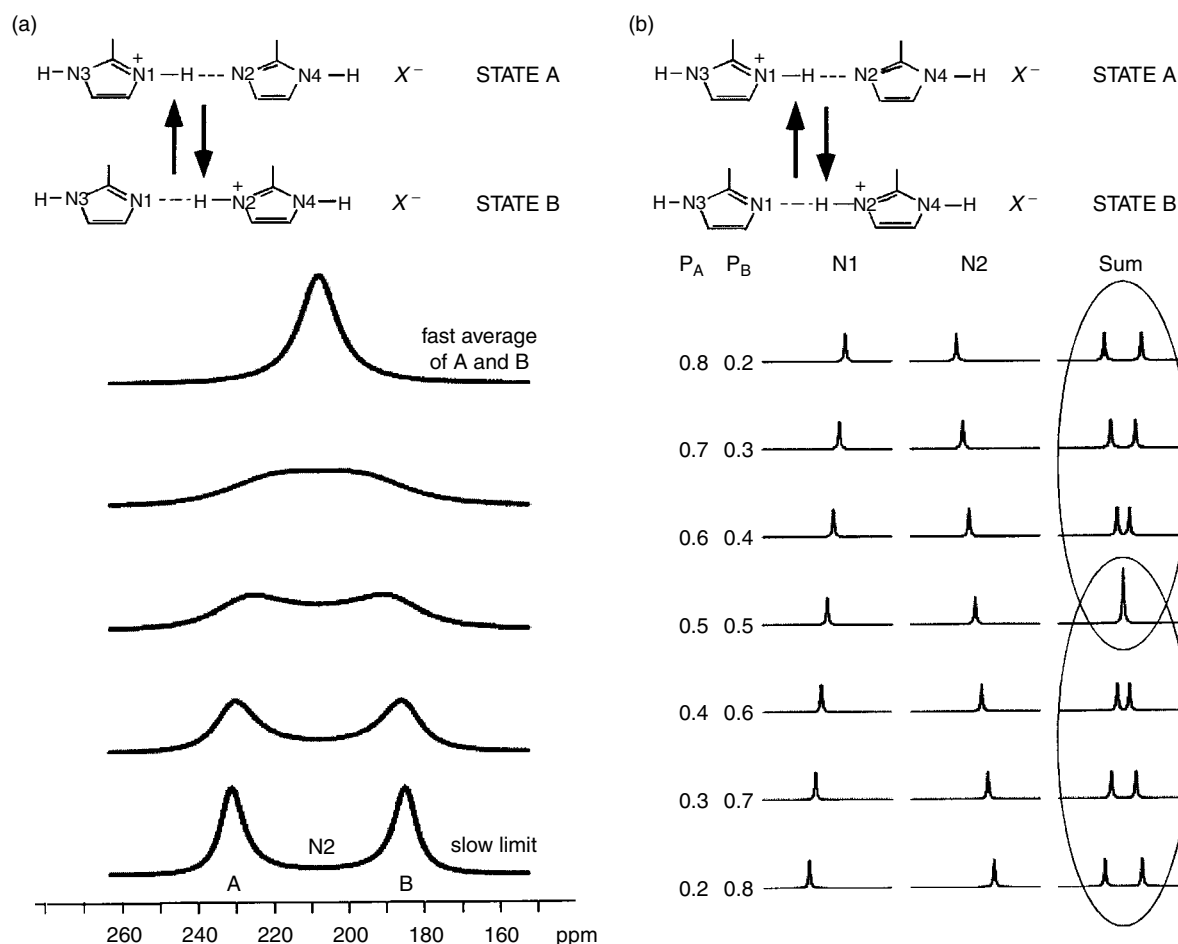


**Figure 2.** (a) Simulated spectra for a proton transfer process through the NHN bridge with intermediate exchange behavior. The simulations assumed  $P_A = P_B = 0.5$ ,  $T_2 = 6.6 \text{ ms}$ ,  $\Delta\nu = 1429.69 \text{ Hz}$  and rate constants ( $k_A$ ) were from bottom to top 500, 1000, 2000, 3000 and  $10000 \text{ s}^{-1}$ . These simulations differ markedly from the experimental data; pronounced broadening is seen in the simulations, which is typical for chemical exchange in the intermediate rate regime, but no such broadening was seen for the experimental data. (b) Simulations for  $^{15}\text{N}$  signals for a population-dependent fast limit proton transfer process involving two otherwise symmetric nitrogen sites in an NHN bridge. The two peaks will apparently coalesce when  $P_A = P_B$ . Simulations assumed  $T_2 = 6.6 \text{ ms}$ ,  $\delta\nu = 1429.69 \text{ Hz}$  and a rate constant of  $5 \times 10^6 \text{ s}^{-1}$ . Populations are strongly dependent on the assumption for  $\delta\nu$ , which can realistically be anywhere from about 1000 to 1500 Hz.

two-site exchange for a system of broken symmetry.<sup>7</sup> Quantitative lineshape analysis clarifies the nature of this proton transfer (specifically the populations, see below) but other qualitative discussion will be described first.

Other NMR data can be used to support the conclusion that the proton transfer is rapid on the NMR time-scale. 2D exchange spectra for these compounds (Fig. 3) do not show chemical exchange cross peaks, whereas spin diffusion cross peaks are seen at long mixing times at all temperatures and allow us to assign the nitrogen spectra. These results suggest that the proton transfer is too fast at higher temperatures to allow the production of chemical exchange cross peaks. Nitrogen spin–lattice relaxation times for the chloride salt (data not shown) are relatively long at all temperatures (>10 s) but do shorten at 200 K (~12 s) compared with room temperature (~25 s). These data are again consistent with the presence of fast limit motion, where at every temperature the rate is substantially faster than the Larmor frequency for <sup>15</sup>N.

Lineshape fitting was used to discern these phenomena more quantitatively, particularly to derive the populations of the two species involved, and estimate the enthalpy of the proton transfer and environment reorganization. In our simulations of the lineshapes, we utilized expressions that are derived from a set of modified Bloch equations.<sup>48</sup> Both rate constants and populations can be considered as variables. The rate constant was in the fast limit throughout the simulation ( $k \gg 10^5 \text{ s}^{-1}$ ).  $T_2$  values were estimated from our experimental data, which show that the linewidths of the two imidazole nitrogen peaks are 45–50 Hz, so that  $T_2 = (\pi \times 48 \text{ Hz})^{-1} \approx 6.6 \text{ ms}$ . The static splitting was derived from our data with some consideration of the previous literature. Practically, we could not measure spectra at temperatures lower than 190 K, and we must consider whether the spectra represent limiting cases of cation and neutral rings at this temperature. The chemical shift difference for the two sites is different at 190 K than it is at 200 K, and thus we cannot argue that the populations have reached a static limit in which one configuration (see the scheme at the top of Fig. 1) is overwhelmingly populated and the other negligibly so. Literature values for nitrogen shifts

in hydrogen-bonded imidazole systems are discussed above (i.e. 230 ppm for the deprotonated state and 185 ppm for the protonated state); our  $pK_a$ -matched NHN model compounds are expected to have even shorter hydrogen bond lengths and the nitrogen shifts might resemble more closely the values for the slow-limit, fully populated perchlorate salt reported here in Table 2 (217 ppm for the deprotonated state and 197 ppm for the protonated state). The shifts observed at 190 K for the chloride and bromide salts (223 ppm for the deprotonated state and 191 ppm for the protonated state) are between these two limits but closer to those of the perchlorate salt. The choice of these chemical shift values is arbitrary on the basis of the available data, and biased the treatment of the temperature-dependent equilibrium constant. We considered two limiting cases for the chloride salts: case 1, that the shifts at 190 K derive from pure imidazole and imidazolium species; and case 2, that the equilibrium constant at this temperature is still non-zero, and the limiting shifts are similar to values from the literature.

Figure 4 shows the simulations of the spectra of (2MI)<sub>2</sub>HCl based on the hypothesis of temperature-dependent populations. Populations listed in the figure correspond to the assumption that the chemical shifts for the limiting species resemble literature values. The population values derived from this simulation (and those under the assumption that the 190 K spectrum corresponds to a population of 1.0 for state B) were used to estimate the enthalpy change in the process, as shown in Fig. 5. If it is assumed that the spectra at 190 K reflect state B only, then an enthalpy of approximately 19 kJ mol<sup>-1</sup> derives from the linear plot of  $\ln K_{eq}$  against  $1/T$ . If instead the populations listed in Fig. 4 are used, then a break in the plot of the equilibrium constant over temperature occurs, and a possible phase transition is implied, where the enthalpy is ~22 kJ mol<sup>-1</sup> at low temperatures and is substantially less and poorly defined at higher temperatures. This enthalpy depends on the anion, and is smaller for the bromide salt. The perchloride sample may have reorganization terms that are even larger, owing to its bulky volume, and for the iodide the reorganization is probably facile.

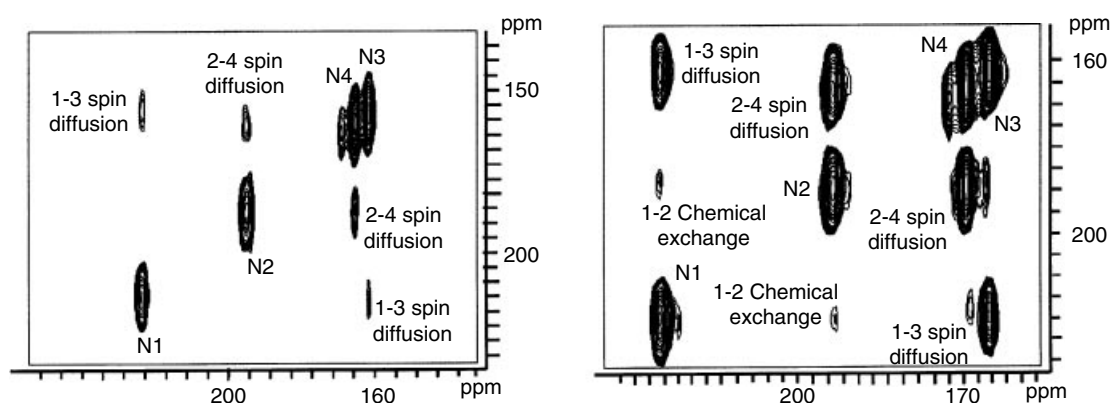


**Figure 3.** 2D exchange spectrum of (2MI)<sub>2</sub>HCl. Left, a spectrum taken with a 300 ms mixing time (4.5 kHz spinning at 230 K); right, a spectrum taken with a 2 s mixing time (4.5 kHz spinning speed at 220 K). The intensities of the putative exchange cross peaks are about 10–15% of the peaks of N-1 and N-2 and can equally well be explained by spin diffusion; the sample consisted of 10% U-labeled Im and 90% natural abundance material. The spin diffusion cross peaks were essentially independent of temperature and could be used to perform peak assignments.

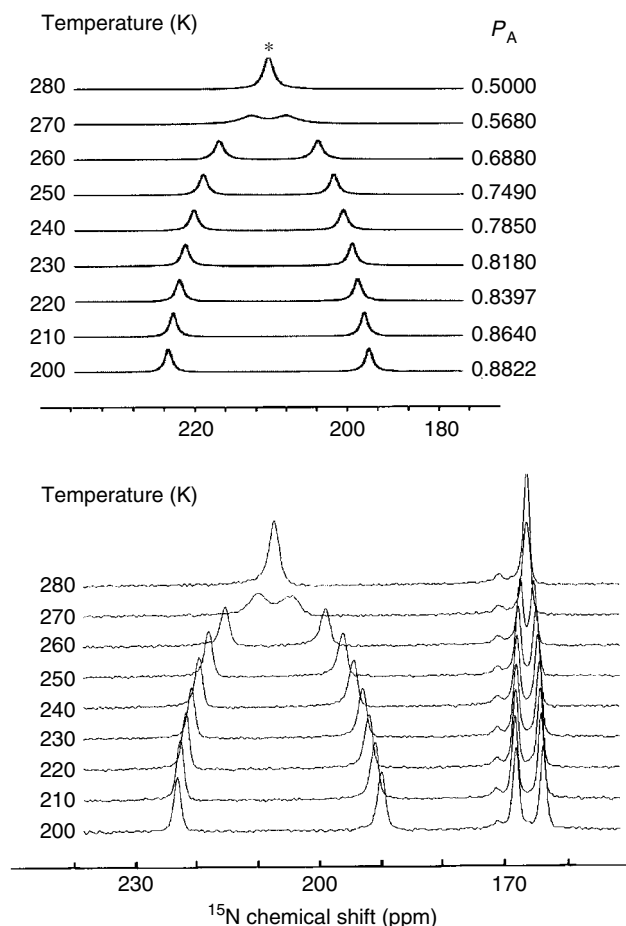


**Figure 4.** Simulated (top) and experimental (bottom) spectra for the temperature-dependent lineshape of a  $(2\text{MI})_2\text{HCl}$  sample. We assumed  $\Delta\nu = 1344.40$  Hz for the protonated and deprotonated forms of the bridging nitrogen.  $T_2$  values were based on the linewidths in Table 2.  $P_A$  values are the population of state A as drawn. The height of the peak marked with an asterisk was reduced for plotting; the peak at 280 K has double the intensity of the separated peaks.

As expected, N—H dipolar bond strengths in these compounds reflect the proton occupancies. The dipolar coupling spinning sideband patterns for the chloride and perchlorate samples were measured using 2D  $2\phi$ -DipShift experiments, and compared with simulations and spectra of other characterized compounds.<sup>33</sup> At low temperatures (210 K) the dipolar strength for the bridging N—H is weak and is consistent with a bond length of  $\sim 1.10$  Å, whereas the dipolar pattern in the outer N—H bonds is consistent with a distance of 1.00 Å. As the chloride sample is warmed, the N,H dipolar coupling for the outer N—H bond is invariant, whereas N,H dipolar coupling for the bridging N—H group becomes noticeably weaker, consistent with the suggestion that the proton occupancy in the bridge varies with temperature.

Although rapid proton transfer in a nearly symmetric hydrogen bond is the norm, it is not always the case. Solid-state reactions can have slower rates than liquid-phase reactions,<sup>32</sup> and proton transfers in NHN hydrogen bonds are often thought to be slower than those in OHO hydrogen

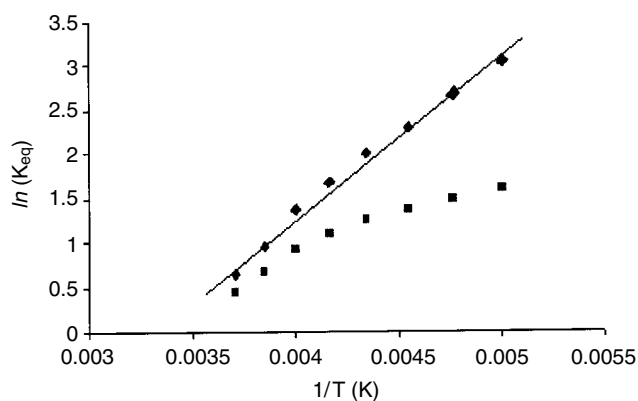


**Figure 5.** Plot of  $\ln K_{\text{eq}}$  versus  $1/T$  ( $\text{K}^{-1}$ ) for the  $(2\text{MI})_2\text{HCl}$  sample, according to the populations obtained from the simulations such as those shown in Fig. 4. Points above (diamonds) derive from the assumption that the process is saturated at 190 K and use chemical shifts for the limiting species derived from that spectrum, and points below (squares) derive from the assumption that the process is not saturated at 190 K and use chemical shift values derived from the literature. The correlation is not linear, but is more closely so if the process is assumed to be saturated at 190 K. Enthalpy values at higher temperatures are similar in either case,  $\Delta H(>250 \text{ K}) \approx 20 \text{ kJ mol}^{-1}$ , and had a correlation coefficient for the higher temperatures of 0.993 in either model. Similar treatment for the HBr salt resulted in lower values ( $18 \text{ kJ mol}^{-1}$  at higher temperatures).

bonds.<sup>49,50</sup> Hence the facile transfer here was not obvious from the outset. It has not been possible to measure rate constants, or to relate this study to the notion of low barrier hydrogen bonds, i.e. establish that the barrier is less the vibrational zero point energy.<sup>51,52</sup> Based on these qualitative results, however, the imidazole model system provides a vivid example of the dependence of the potential barrier on the ionic environment.

## CONCLUSIONS

$[2\text{-MeIm}_2\text{H}]^+\text{X}^-$  salts have been shown to form short N—H...N hydrogen bonds in the crystalline state.  $^{15}\text{N}$  NMR spectra indicate that the proton transfer processes can be facile for these compounds, even at low temperatures. The N,H dipolar coupling patterns for the two NHN nitrogens also support a skewed population of two exchanging states at low temperatures. Although the N...N distances are similar for the four samples, counter ions caused the equilibrium constant for the proton transfer reaction to vary substantially.

## Acknowledgments

We thank Professor Ged Parkin and Dr Brian Bridgewater for their generous and expert assistance with the x-ray diffraction studies. Support was provided by the National Institutes of Health, GM49964.

## REFERENCES

1. Golubev NS, Denisov GS, Gindin VA, Ligay SS, Limabach H-H. *J. Mol. Struct.* 1994; **322**: 83.

2. Tong L, Qian C, Massariol M-J, Bonneau PR, Cordingley MG, Lagace L. *Nature (London)* 1996; **383**: 272.
3. Stefaniak L. *Poli. J. Chem.* 1998; **73**: 173.
4. Klimkiewicz J, Stefaniak L, Grech E, Brzezinski B, Webb GA. *Bull. Pol. Acad. Sci. Chem.* 1997; **46**: 1998.
5. Malarski Z, Sobczyk L. *J. Mol. Struct.* 1988; **177**: 339.
6. Brycki B, Brzezinski B. *Magn. Reson. Chem.* 1991; **29**: 558.
7. Glowiak T, Grech E, Malarski Z, Nowicka-Scheibe J, Sobczyk L. *J. Mol. Struct.* 1996; **381**: 169.
8. Bar E, Fuchs J, Rieger D, Aguilar-Parrilla F, Limbach H-H, Fehllhammer WP. *Angew. Chem. Int. Ed. Engl.* 1991; **30**: 88.
9. Benedict H, Limbach H-H, Wehlan M, Fehllhammer W-P, Golubev NS, Janoschek R. *J. Am. Chem. Soc.* 1998; **120**: 2939.
10. Brammer L, Zhao D. *Acta Crystallogr., Sect. C* 1994; **51**: 45.
11. Quick A, Williams DJ. *Can. J. Chem.* 1975; **54**: 2465.
12. Bock H, Vaupel T, Schodel H, Koch U, Egert E. *Tetrahedron Lett.* 1994; **35**: 7355.
13. Therrien B, Beauchamp AL. *Acta Crystallogr., Sect. C* 1992; **49**: 1303.
14. Akutagawa T, Saito G, Kusunoki M, Sakaguchi K-i. *Bull. Chem. Soc. Jpn.* 1996; **69**: 2487.
15. Higgs TC, Helliwell M, Garner D. *J. Chem. Soc. Dalton Trans.* 1996; 2101.
16. Jeffrey GA, Saenger W. *Hydrogen Bonding in Biological Structures*. Springer: Berlin, 1991.
17. McDermott A, Wei Y. *Modeling of NMR Chemical Shifts*. American Chemical Society: Washington, DC, 1999.
18. Steiner T. *J. Chem. Soc. Chem. Commun.* 1995; 1331.
19. Steiner T. *J. Phys. Chem. A* 1998; **102**: 7041.
20. Bartoszak E, Dega-Szafran Z, Jaskolski M, Szafran M. *J. Chem. Soc. Faraday Trans.* 1995; **91**: 87.
21. Klimskiewicz J, Koprowski M, Stefaniak L, Grech E, Webb GA. *J. Mol. Struct.* 1996; **403**: 163.
22. Scheiner S. *J. Mol. Struct. (Theochem)* 1994; **307**: 65.
23. Scheiner S, Duan X. *Biophys. J.* 1991; **60**: 874.
24. Scheiner S. *Acc. Chem. Res.* 1994; **27**: 402.
25. Therrien B, Beauchamp AL. *Acta Crystallogr., Sect. C* 1993; **49**: 1303.
26. Bennett AE, Rienstra CM, Auger M, Lakshmi KV, Griffin RG. *J. Chem. Phys.* 1995; **103**: 6951.
27. Jeener J, Meier BH, Bachmann P, Ernst RR. *J. Chem. Phys.* 1979; **71**: 4546.
28. Perrin CL, Dwyer T. *J. Chem. Rev.* 1990; **90**: 935.
29. Harbison GS, Raleigh DP, Herzfeld J, Griffin RG. *J. Magn. Reson.* 1985; **64**: 284.
30. Kentgens APM, de Jong AF, de Boer E, Veeman WS. *Macromolecules* 1985; **18**: 1045.
31. Tycko R, Weiliky DP, Berger AE. *J. Chem. Phys.* 1996; **105**: 7915.
32. Szeverenyi NM, Sullivan MJ, Maciel GE. *J. Magn. Reson.* 1982; **47**: 462.
33. Song X-j. PhD, Thesis Columbia University, New York, 2000.
34. Munowitz MG, Griffin RG, Bodenhausen G, Huang TH. *J. Am. Chem. Soc.* 1981; **103**: 2529.
35. Munowitz MG, Griffin RG. *J. Chem. Phys.* 1982; **76**: 2848.
36. Roberts JE, Harbison GS, Munowitz MG, Herzfeld J, Griffin RG. *J. Am. Chem. Soc.* 1987; **109**: 4163.
37. Ernst RR, Bodenhausen G, Wokaun A. *Principles of NMR in One and Two Dimensions*. Clarendon Press: Oxford, 1990.
38. Hong M, Gross JD, Rienstra CM, Griffin RG, Kumashiro KK, Schmidt-Rohr K. *J. Magn. Reson.* 1997; **129**: 85.
39. Smith SO, Farr-Jones S, Griffin RG, Bachovchin WW. *Science* 1989; **244**: 961.
40. Wei Y. PhD Thesis, Columbia University, New York, 1999.
41. Bachovchin WW. *Biochemistry* 1986; **25**: 7751.
42. Brickmann VJ, Zimmermann H. *Ber. Bun. Ges.* 1967; **70**: 521.
43. Borgis D. In *Electron and Proton Transfer in Chemistry and Biology*, Muller A, Ratajczak H, Junge W, Diemann E (eds). Elsevier: Amsterdam, 1992.
44. Scheiner S. *J. Mol. Struct. (Theochem)* 1993; **307**: 65.
45. Wehrle B, Limbach H-H. *Chem. Phys.* 1989; **136**: 223.
46. Wehrle B, Zimmermann H, Limbach H-H. *J. Am. Chem. Soc.* 1988; **110**: 7014.
47. Wehrle B, Limbach H-H, Zimmermann H. *Ber. Bunsenges. Phys. Chem.* 1987; **91**: 941.
48. Sandstrom J. *Dynamic NMR Spectroscopy*. Academic Press: New York, 1982.
49. Eyring EM, Marshall DB, Strohbusch F. *ACS Symp. Ser.* 1982; **198**: 403.
50. Limbach H-H, Wehrle B, Zimmermann H, Kendrick RD, Yan-noni CS. *Angew. Chem. Int. Ed. Engl.* 1987; **26**: 247.
51. Cleland WW. *Biochemistry* 1992; **31**: 317.
52. Cleland WW, Kreevoy MM. *Science* 1994; **264**: 1887.